CARBON 49 (2011) 4781–4785

available at www.sciencedirect.com

ScienceDirect

journal homepage: www.elsevier.com/locate/carbon

Ultrafast modulation of optical transitions in monolayer and multilayer graphene

Ki-Ju Yee [a,d,*], Ji-Hee Kim [a], Myung Hee Jung [b], Byung Hee Hong [b], Ki-Jeong Kong [c]

[a] Department of Physics and Center for Subwavelength Optics, Chungnam National University, Daejeon 305-764, Republic of Korea
[b] Department of Chemistry & SKKU Advanced Institute of Nanotechnology, Sungkyunkwan University, Suwon 440-746, Republic of Korea
[c] Korea Research Institute of Chemical Technology, Daejeon 305-600, Republic of Korea
[d] GRAST, Chungnam National University, Daejeon 305-764, Republic of Korea

ARTICLE INFO

Article history:
Received 25 February 2011
Accepted 25 June 2011
Available online 30 June 2011

ABSTRACT

We study ultrafast modulations of absorption spectra for both monolayer and multilayer graphene, by performing time-resolved transmission measurements with tuning probe photon energy. While reduced absorptions by photo-excited carriers are observed in monolayer graphene irrespective of the probe energy, multilayer graphene shows increased absorption at around 0.6 eV, which is explained by the optical transitions between subband states. Intraband carrier relaxation and electron–hole recombination times are found to be as fast as 0.5 and 10 ps, respectively. Modifications of ultrafast carrier dynamics are also studied with changing temperature and excitation density.

1. Introduction

A discovery of graphene from mechanical exfoliation has stimulated explosive research in both fundamentals and applications [1,2]. Together with unique electronic properties, interesting optical properties of graphene such as 2.3% opacity per single atomic layer and gate-variable optical transitions, have enabled it to be pursued toward nano-photonic applications [3,4]. High-speed photodetector from graphene relies on high carrier mobility of massless Dirac fermions, which enables photo-generated carriers to reach electrodes before recombination process occurs [5]. Graphene saturable absorber applied in femtosecond lasers relies on ultrafast carrier relaxation within linear Dirac cones [6,7]. These graphene-based photonic devices can have ultra-broad spectral bandwidth from terahertz to visible while band gap energy sets spectral limits for conventional semiconductor photonic devices [8].

Monolayer graphene has conical linear electron bands near the *K* point in reciprocal space, with forming massless Dirac fermions. As more layers are stacked, the structural and electronic properties approach to those of three dimensional graphite with an ABAB Bernal interlayer structure weakly bonded between layers [9,10]. Although monolayer graphene has appreciable optical interactions, attainable by a semiconductor of the order of 10 nm thick, use of multilayer graphene is more practical in increasing the interaction efficiency with photons [5–7]. Since the electron energy dispersion deviates from that of monolayer graphene due to the interlayer coupling, some kind of optical activities are expected to occur exclusively in multilayer graphene.

In this paper, we describe on transient absorptions induced by photoexcited carriers in graphene, especially for the photon energy on resonance with the inter-subband transitions of multilayer graphene. The induced absorptions observed for the multilayer but not for the monolayer

* *Corresponding author at:* Department of Physics and Center for Subwavelength Optics, Chungnam National University, Daejeon 305-764, Republic of Korea. Fax: +82 42 822 8011.
E-mail address: kyee@cnu.ac.kr (K.-J. Yee).
0008-6223/$ - see front matter
doi:10.1016/j.carbon.2011.06.088

graphene arose from an intersubband optical transition and provide an evidence for the multiple subbands within the valence band (VB) or the conduction band (CB). The dependence of carrier relaxation on temperature and carrier concentration was also examined.

2. Experimental

In the pump–probe experiments, pump pulse excite carriers with inducing transient electronic and optical changes within the sample, and the subsequent dynamical process that electrons recover to the equilibrium states is studied by measuring reflection or transmission of the probe pulses with sweeping the time delay between pump and probe pulses. After the interband carrier generation by pump pulses from a Ti:sapphire laser having a duration of 100 fs and a center energy of 1.56 eV, transient absorptions at tunable probe energies from 0.4 to 1.2 eV were measured as a function of the time delay between pump and probe pulses. The probing photons were obtained from an optical parametric oscillator that generates signal photons in the range from 1.0 to 1.6 μm and idler photons from 1.6 to 3.0 μm [11]. Pump photons elevate the valence electrons to the CB, launching non-thermal and highly energetic electrons/holes into states above/below, respectively, the Dirac point by half the photon energy in monolayer graphene. The excited carrier density was varied up to 5.2×10^{10} cm^{-2} per layer. Most measurements were performed at 80 K, and the temperature was varied from 80 to 300 K for a temperature-dependent study.

Two different epitaxial samples were compared; one is a single layered graphene with 95% monolayer coverage, and the other is a multilayer graphene with an average layer number of around 10. Graphene layers were synthesized by chemical vapor deposition (CVD) on Cu foils or Ni films [12,13]. After spin-coating the graphene films with 5 wt.% polymethylmethacrylate (PMMA) in chlorobenzene, the underlying Cu or Ni layers were etched. The graphene layers with PMMA were transferred onto quartz substrates, and the PMMA layer was then removed by acetone. As is observed from the Raman spectra in Fig. 1, the energy shift of the G-mode and the relative intensity ratio are distinct features that permitted discrimination between the monolayer and multilayer graphene. Transmission electron microscopy (TEM) images in the inset of Fig. 1 also show that the graphene film grown on Cu is a monolayer without noticeable defects or contaminations, whereas the number of graphene layers grown on Ni is around 10.

3. Results and discussion

Fig. 2 shows time-resolved transmission changes for the monolayer graphene at different probe energies. Photo excited carrier density was around 3.5×10^{10} cm^{-2}, and sample temperature was 80 K. Bi-exponential decay of the signal indicates multiple steps in the carrier dynamics. The fast component is generally assigned to the thermalization process through carrier–carrier scatterings, during which carriers reach Fermi–Dirac distributions at elevated temperatures. Cooling of the carrier temperature through interactions with

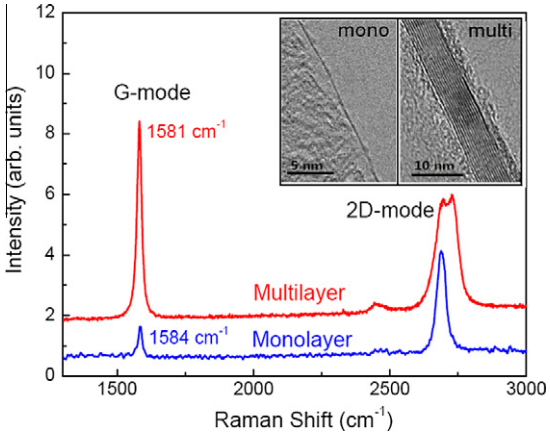

Fig. 1 – Raman spectrum for monolayer graphene synthesized on Cu foil and that for multilayer graphene synthesized on Ni film by CVD method. Insets are TEM images for the monolayer and the multilayer graphene.

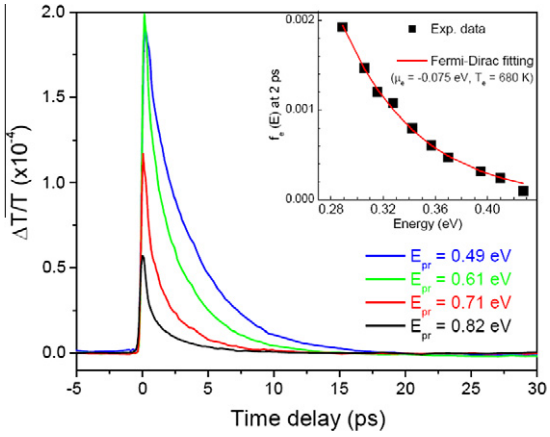

Fig. 2 – Time-resolved transmission changes for the monolayer graphene at different probe energies. The inset shows electron occupations at time delay of 2 ps as a function of energy, calculated from transient transmissions (solids) and the corresponding fitting curve with the Fermi–Dirac function (line).

the lattice is known as the origin of the slower dynamics [14–18]. The overall increase in the signal with decreased probe energy testifies the larger occupation probability by electrons or holes at states close to the Dirac point. Strong initial signal, even for probe energies 1 eV less than the pump photon, supports the ultrafast intraband carrier thermalization process that is possibly beyond our temporal resolution [15,19].

Positive transmission change results from the effect of photo-bleaching, in which both the depletion of the valence electrons (hole) and the electron occupation at the CB, induced by the pump pulse, reduce the interband optical transition probability of the probe pulse. The absorption probability at ω by Fermi's golden rule will be proportional to the product of the valence band electron occupation at $-\frac{\omega}{2}$ with $1 - f_h(-\frac{\omega}{2})$ and the conduction band electron vacancy

at $\frac{\omega}{2}$ with $1 - f_e(-\frac{\omega}{2})$, which leads to Eq. (1) at low excitation regime of $f_e(\frac{\omega}{2})$, $f_h(-\frac{\omega}{2}) << 1$.

$$\alpha(\omega) \approx \alpha_0(\omega) \times [1 - f_e(\omega/2) - f_h(-\omega/2)] \quad (1)$$

$\alpha_0(\omega)$, $\alpha(\omega)$ $f_e(\frac{\omega}{2})$ and $f_h(-\frac{\omega}{2})$ represent absorption probability without excited carriers, absorption probability after carrier excitation, electron occupation at conduction band, and hole occupation at valence band, respectively. When the absorption probability is low, which is the case for monolayer graphene, the transmission T can be approximated to $(1 - \alpha \times l)$ with l being an effective length of the material. Thus, the relative transmission change $(T - T_0)/T_0 = \Delta T/T_0$ induced by the carrier excitation, with T_0 being transmission before carrier excitation, will be proportional to $-(\alpha(\omega) - \alpha_0(\omega)) \times l$, where $\alpha_0(\omega) \times l$ is known to be 0.023 in the region of our interests for monolayer graphene [3]. Assuming the same behavior of electrons and holes with $f_e(\omega/2) = f_h(-\omega/2)$, the electron occupation can be obtained from a relative transmission change, such that,

$$f_e(\omega/2) \approx \frac{\Delta T/T_0(\omega)}{2 \times 0.023}. \quad (2)$$

The scatters in the inset of Fig. 2 depict the electron occupations after 2 ps of carrier excitations as a function of the electron energy, which were obtained from relative transmission changes following Eq. (2). With fitting the data by Fermi–Dirac distribution of $f_e(E) = 1/[1 + \exp(E - \mu_e)/kT_e]$, we find that thermal distribution with the electron chemical potential of $\mu_e = -75$ meV and the electron temperature of $T_e = 680$ K is reached at the time delay of 2 ps. We note that the initial transmission change at probe energy of 0.61 eV is larger than that of 0.49 eV near zero time delay, which contradicts to the expectations from the Fermi–Dirac carrier distributions. We think that this discrepancy results from delayed establishment of thermal distribution for low energy states, such that the signal at 0.49 eV becomes larger than that at 0.61 eV after 0.3 ps, with the thermal distribution is being approached.

In contrast to the monolayer graphene, pump-induced absorption changes for the multilayer graphene, shown in Fig. 3, depend strongly on the probe photon energy. The most distinct difference appears for probe energies near 0.6 eV, at which the initially positive signal transits to a negative maximum within less than 0.5 ps, with followed by an exponential decay of the negative signal. The signal strength at time delay of 2 ps is shown as a function of the probe energy in the inset of Fig. 3. Because our graphene layers were translated on insulating glass, and monolayer graphene does not show such behavior, we can exclude the effect of doping from the origin of negative transmission changes [16].

To elucidate the energy dependent transient absorptions in multilayer graphene, we have simulated the modification of absorptions by photo-excited carriers. As is shown in Fig. 4(a), electron energy bands were calculated for multilayer graphene with $n = 10$, by using first principles calculations with plane wave based density functional method. Whereas monolayer graphene features a linear band near the K point, multiple subbands as many as the layer number constitute the energy states for the multilayer graphene. Half the subbands closely overlap near the Dirac point (upper VBs, lower CBs) and the others are dispersed with considerable energy

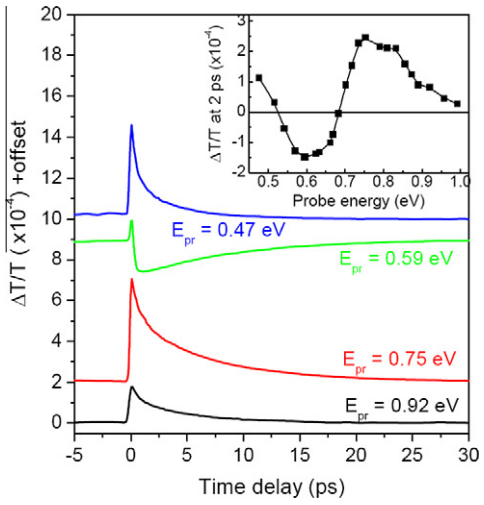

Fig. 3 – Time-resolved transmission changes at several probe energies for the multilayer graphene. The inset shows signal amplitude at time delay of 2 ps as a function of probe energy.

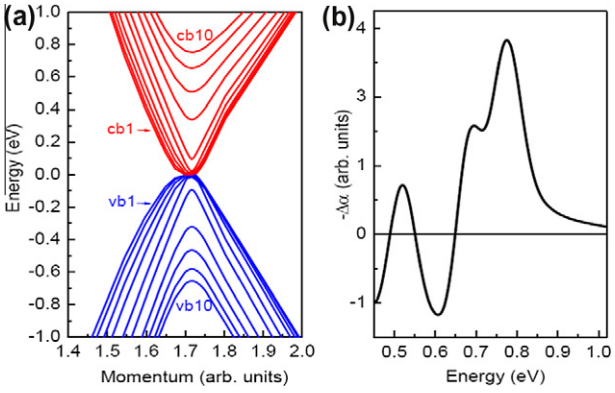

Fig. 4 – (a) Energy band dispersions near the K-point of the Brillouin zone for the multilayer graphene with 10 layers, which were calculated from the first principles method. Cb1, cb10, vb1, and vb10 denote 1st conduction subband, 10th conduction subband, 1st valence subband, and 10th valence subband, respectively. (b) Simulated modification of the absorption spectrum induced by photoexcited carriers in multilayer graphene.

gaps (upper CBs, lower VBs). From the existence of multiple subbands in multilayer graphene, it is necessary to consider optical transitions from a subband to another subband.

As photoexcited carriers are accumulated at states near the Dirac point, the probability of the inter-subband optical transitions corresponding to the excitation of the relaxed carriers to higher subband states will be increased. Fig. 4(b) shows calculated difference between the absorption spectrum at electron distributions before excitation ($\mu_e = 0$ eV, $T_e = 80$ K) and that at 2 ps ($\mu_e = -0.075$ eV, $T_e = 680$ K) after excitation, where we have assumed that the initial electron distribution after photoexcitation is similar between monolayer and multilayer graphene. We note that slight deviation

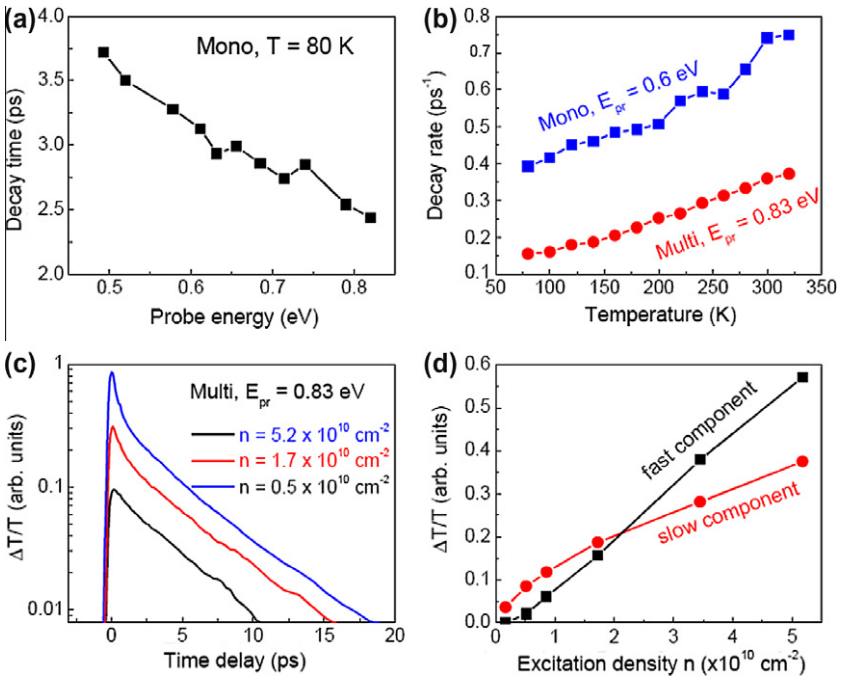

Fig. 5 – (a) Decay time of the slow component with probe energy, measured for the monolayer graphene at 80 K. (b) Decay rate of the slow signal as a function of temperature for both the monolayer and the multilayer graphene. (c) Excitation density dependence of the time-resolved absorption signal for the multilayer graphene at a probe energy of 0.83 eV. (d) The initial amplitudes of the fast and the slow component as a function of excitation density.

of electron distribution from the assumed values does not change spectral features of transient absorptions for the multilayer graphene. For simplicity of calculations, oscillator strength for each direct transition was assumed to be identical, and any indirect optical transition was neglected. The calculation of the differential absorption successfully reproduces the induced absorption at around 0.6 eV by the contribution of inter-subband transitions. Rather complicated spectrum in Fig. 4(b) has resulted from a superposition between the photo-bleaching and the inter-subband transitions. At energies lower than 0.5 eV, the simulation deviates from the experimental results, which may have resulted from the simplified assumption of identical oscillator strength irrespective of energy states. We note that the oscillator strength is actually stronger for transitions between states closer to Dirac points [3].

The positive initial transmission change even at a probe energy of 0.59 eV, which is clear in Fig. 3, can be understood as an initial dominance of the photo-bleaching effect before the excited carriers relax to occupy the lower conduction or upper valence subband states. The positive-to-negative signal transition occurring within 0.5 ps, thus confirms ultrafast establishment of the Fermi–Dirac carrier distribution. Exponential decay of the negative signal with being fitted by a decay time 8.7 ps, demonstrates that perturbed carrier distribution recovers within 10 ps through electron–hole recombination and carrier-phonon scatterings.

Further dynamic carrier relaxations were analyzed by measuring transient absorptions as functions of temperature and excitation density. Faster signal decays at higher probe energies are apparent, as shown in Fig. 5(a) for the monolayer graphene. This trend arose from the gradual intraband carrier relaxations along the linear energy band, where the effective lifetimes at lower energy states will be elongated due to carrier relaxations from upper energy states.

Fig. 5(b) displays decay rates as a function of temperature. The increased decay rate with temperature can be explained in terms of the carrier relaxations mediated by phonons [20]. The slower carrier relaxation in multilayer graphene, relative to the monolayer, may have resulted from the multiple subbands, such that electrons tend to stay longer at bottom edges of each subbands in multilayer graphene because of relatively slower inter-subband relaxation rate than the intraband carrier relaxation [21]. A double exponential decay is evident at high excitation densities, as is shown in Fig. 5(c) for multilayer graphene. The amplitudes of fast and slow components were obtained by fitting $\Delta T/T$ curves in the range from 0.2 to 20 ps with double exponentially decaying functions and extrapolating the fitting curves to time delay zero. The sublinearity of the slow component with excitation density, as compared to the linear increase of the fast signal, is displayed in Fig. 5(d). We note that the slow component reflecting the thermalized carrier distribution, can be sublinear because the density of states is low as the electron energy approaches the Dirac point. We note that negligible change of the decay time with carrier density contradicts to theoretical predictions expecting intensity-dependent carrier relaxations due to Auger processes or phonon scatterings [22].

4. Conclusion

We report on the observation of different transmission modulations by photoexcited carriers between monolayer and multilayer graphene. While reduced absorption from the

photo-bleaching effect is observed irrespective of the probe energy in monolayer graphene, the induced absorption was measured in multilayer graphene when photon energy was around 0.6 eV, which was interpreted by the inter-subband optical transitions of thermalized electrons. By analyzing the transient transmission signal at the probe energy showing strong induced absorption (0.59 eV), the intra-band carrier relaxation and the electron–hole recombination were found to occur within 0.5 and 10 ps, respectively. Modification of the carrier dynamics in graphene was also studied with varying the excitation density and the sample temperature.

Acknowledgements

This work was supported by the National Research Foundation of Korea (NRF) Grants funded by the Ministry of Education, Science and Technology of Korea (MEST) (2009-0085432, 2010-0001859), a grant from the MEST (2009-008146), the Converging Research Center Program through the MEST (2010K001105), and the R&D program for Energy Efficiency & Resources of the Korea Institute of Energy Technology Evaluation and Planning (KETEP) grant funded by the Ministry of Knowledge Economy, Korea. B.H.H. acknowledges supports from the NRF funded the MEST (2010K001066, 2011-0017587, 2011-0006268).

REFERENCES

[1] Novoselov KS, Geim AK, Morozov SV, Jiang D, Zhang Y, Dubonos SV, et al. Electric Field Effect in Atomically Thin Carbon Films. Science 2004;306(16):666–9.
[2] Zhang Y, Tan YW, Stormer HL, Kim P. Experimental observation of the quantum Hall effect and Berry's phase in graphene. Nature 2005;438:201–4.
[3] Nair RR, Blake P, Grigorenko AN, Novoselov KS, Booth TJ, Stauber T, et al. Fine structure constant defines visual transparency of Graphene. Science 2008;320:1308.
[4] Wang F, Zhang Y, Tian C, Girit C, Zettl A, Crommie M, et al. Gate-variable optical transitions in Graphene. Science 2008;320:206–9.
[5] Xia F, Mueller T, Lin YM, Valdes-Garcia A, Avouris P. Ultrafast graphene photodetector. Nat Nanotechnol 2009;4(12):839–43.
[6] Bao Q, Zhang H, Wang Y, Ni Z, Yan Y, Shen ZX, et al. Atomic-Layer Graphene as a Saturable Absorber for Ultrafast Pulsed Lasers. Adv Funct Mat 2009;19(19):3077–83.
[7] Sun Z, Hasan T, Torrisi F, Popa D, Privitera G, Wang F, et al. Graphene Mode-Locked Ultrafast Laser. ACS Nano 2010;4(2):803–10.
[8] Keller U, Weingarten KJ, Kartner FX, Kopf D, Braun B, Jung ID, et al. Semiconductor saturable absorber mirrors (SESAM's) for femtosecond to nanosecond pulse generation in solid-state lasers. IEEE J Sel Top Quantum Electron 1996;2(3):435–53.
[9] Gupta A, Chen G, Joshi P, Tadigadapa S, Eklund PC. Raman Scattering from high-frequency phonons in supported *n*-Graphene layer films. Nano Lett 2006;6(12):2667–73.
[10] Partoens B, Peeters FM. From graphene to graphite: electronic structure around the K point. Phys Rev B 2006;74:075404 (7).
[11] Han KJ, Jang DW, Kim JH, Min CK, Joo TH, Lim YS, et al. Synchronously pumped optical parametric oscillator based on periodically poled MgO-doped lithium niobate. Opt Express 2008;16(8):5299–304.
[12] Bae S, Kim HK, Lee Y, Xu X, Park JS, Zheng Y, et al. Roll-to-roll production of 30-inch graphene films for transparent electrodes. Nat Nanotechnol 2010;5(8):574–8.
[13] Kim KS, Zhao Y, Jang H, Lee SY, Kim JM, Kim KS, et al. Large-scale pattern growth of graphene films for stretchable transparent electrodes. Nature 2009;457:706–10.
[14] Dawlaty JM, Shivaraman S, Chandrashekhar M, Rana F, Spencer MG. Measurement of ultrafast carrier dynamics in epitaxial graphene. Appl Phys Lett 2008;92:042116 (4).
[15] Breusing M, Ropers C, Elsaesser T. Ultrafast Carrier Dynamics in Graphite. Phys Rev Lett 2009;102:086809 (8).
[16] Sun D, Wu ZK, Divin C, Li X, Berger C, de Heer WA, et al. Ultrafast relaxation of excited dirac fermions in epitaxial graphene using optical differential transmission spectroscopy. Phys Rev Lett 2008;101(15):157402.
[17] Newson RW, Dean J, Schmidt B, van Driel HM. Ultrafast carrier kinetics in exfoliated graphene and thin graphite films. Opt Express 2009;17(4):2326–33.
[18] George PA, Strait J, Dawalth J, Shivaraman S, Chandrashekhar M, Rana F, et al. Ultrafast optical-pump terahertz-probe spectroscopy of the carrier relaxation and recombination dynamics in Epitaxial Graphene. Nano Lett 2008;8(12):4248–51.
[19] Xing G, Guo H, Zhang X, Sum TC, Hon C. The Physics of ultrafast saturable absorption in graphene. Opt Express 2010;18(5):4564–73.
[20] Yu P, Cardona M. Fundamentals of Semiconductors: Physics and Materials Properties. NewYork: Springer; 2005.
[21] Seilmeier A, Hubner KJ, Abstreiter G, Weimann G, Schlapp W. Intersubband relaxation in GaAs–AlxGa1–xAs quantum well structures observed directly by an infrared bleaching technique. Phys Rev Lett 1987;59(12):1345–8.
[22] Rana F, George PA, Strait JH, Dawlaty J, Shivaraman S, Chandrashekhar M, et al. Carrier recombination and generation rates for intravalley and intervalley phonon scattering in graphene. Phys Rev B 2009;79(11):115447.